図10 MNU投与により誘発された胸腺リンパ腫のゲノムDNAを用いた
aCGH解析による*c-Myc*を含む15番染色体の増幅

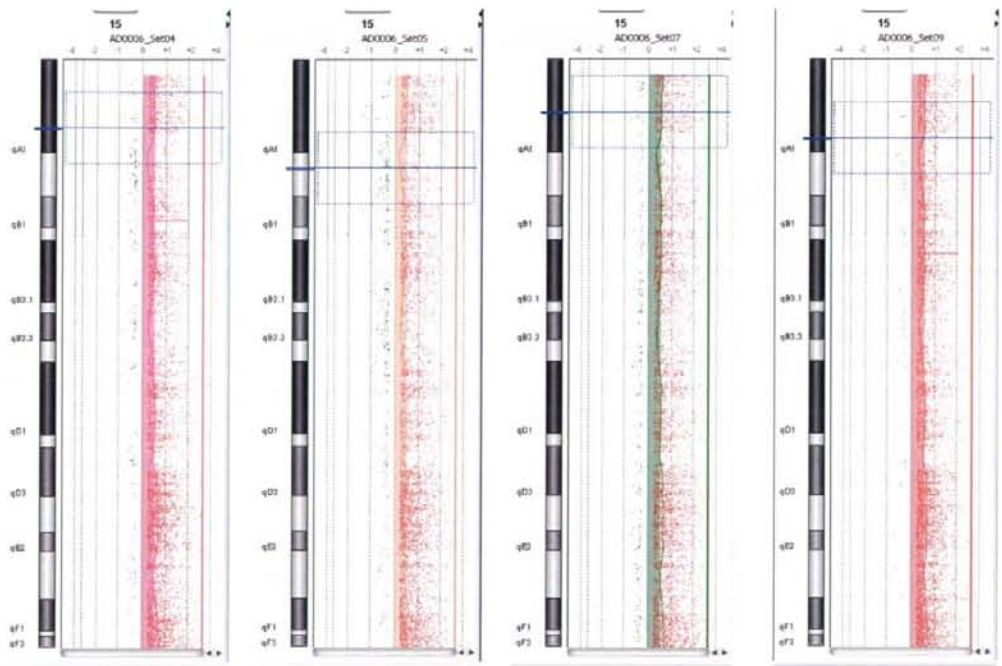

図11　MNU投与により誘発された胸腺リンパ腫のゲノムDNAを用いた
aCGH解析による*TCRβ*を含む6番染色体qB1の欠失

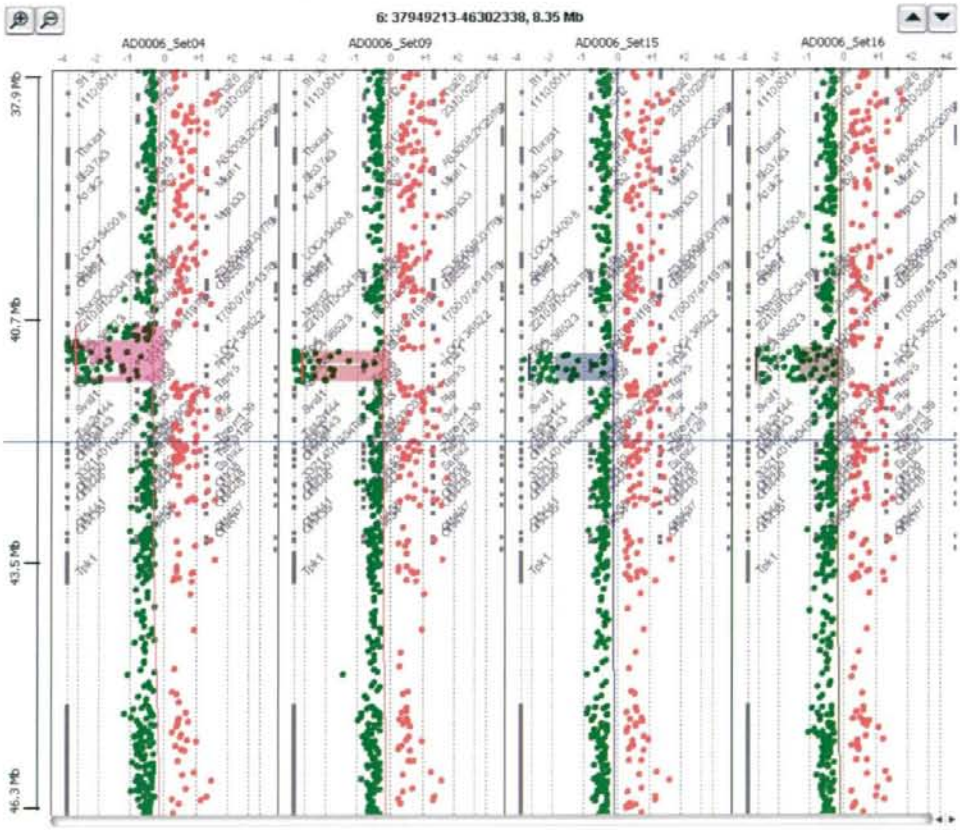

図12　MNU投与により誘発された胸腺リンパ腫のゲノムDNAを用いた
aCGH解析による14番染色体qC1の欠失

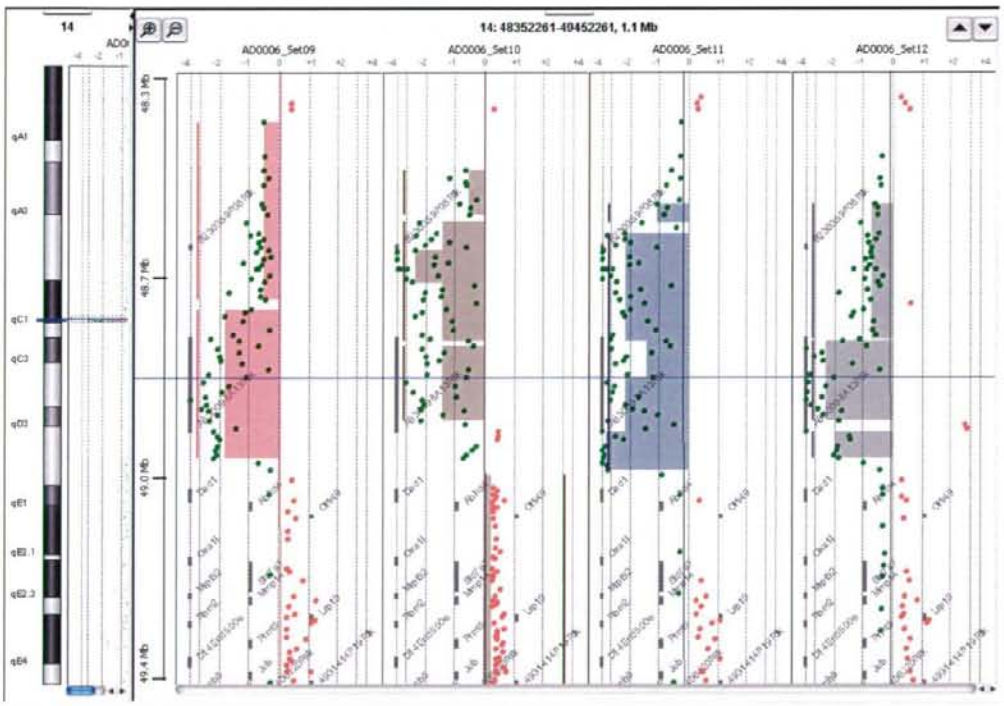

図13-1 雄*Rev1*ホモマウスの体重の推移(ばい煎ダイズ抽出物の1年間反復投与毒性試験)

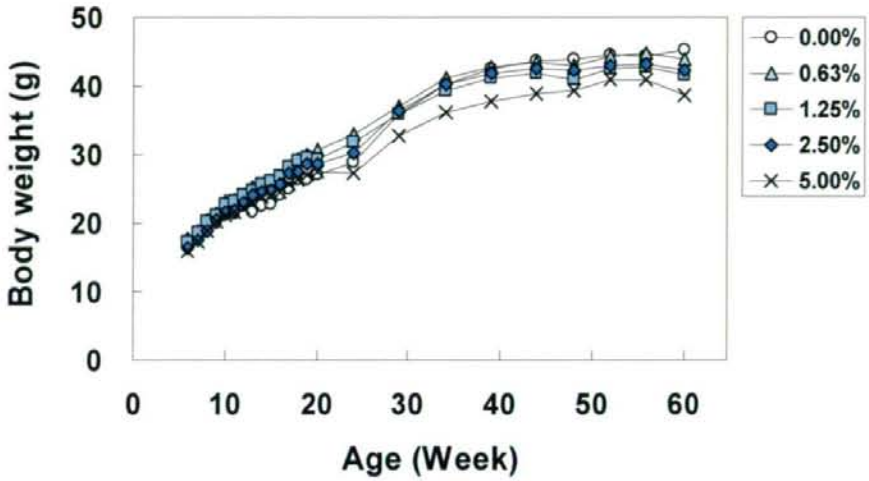

図13-2 雌*Rev1*ホモマウスの体重の推移(ばい煎ダイズ抽出物の1年間反復投与毒性試験)

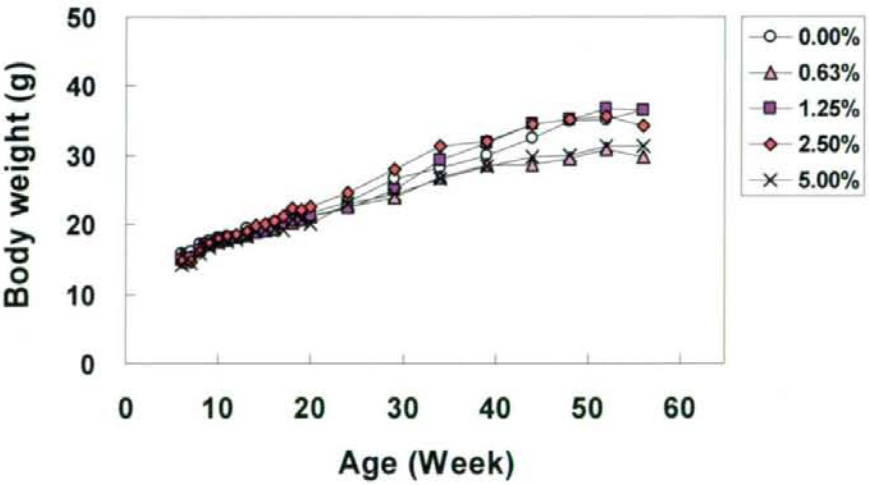

図14-1 雄*Rev1*ホモマウスの平均摂餌量(ばい煎ダイズ抽出物の1年間反復投与毒性試験)

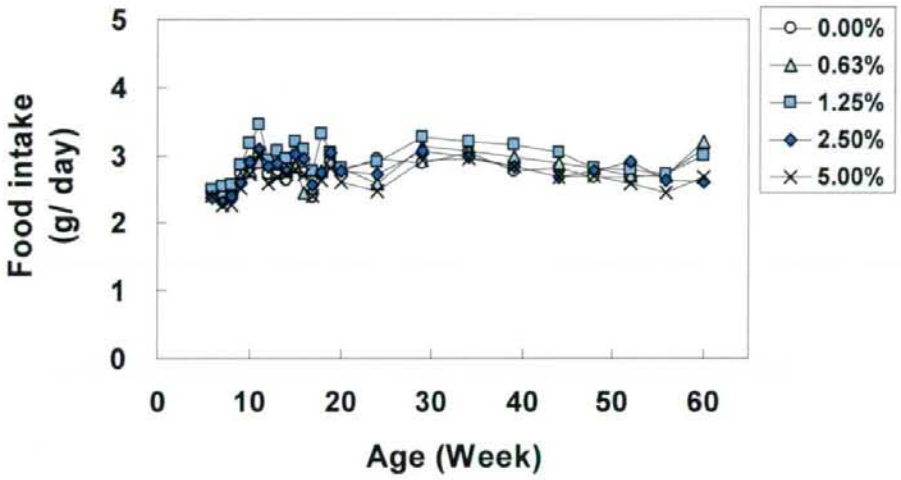

図14-2 雌*Rev1*ホモマウスの平均摂餌量(ばい煎ダイズ抽出物の1年間反復投与毒性試験)

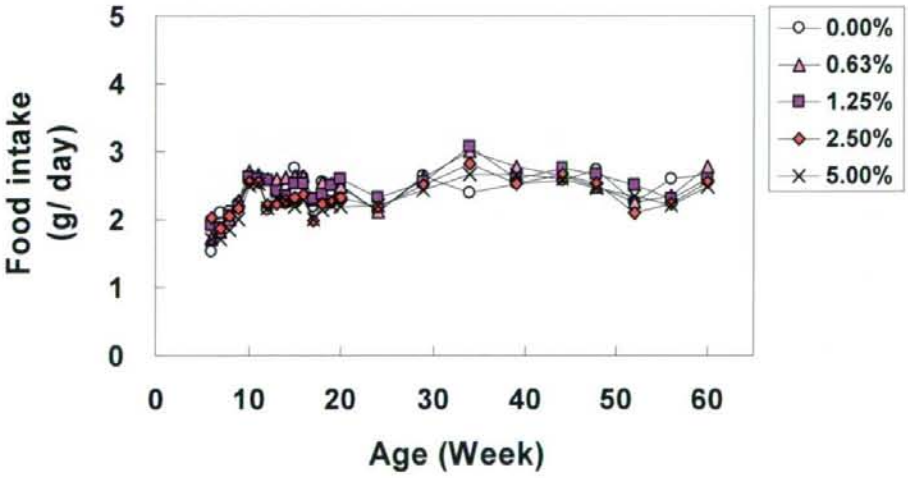

図15-1 雄*Rev1*ホモマウスの平均摂水量(ばい煎ダイズ抽出物の1年間反復投与毒性試験)

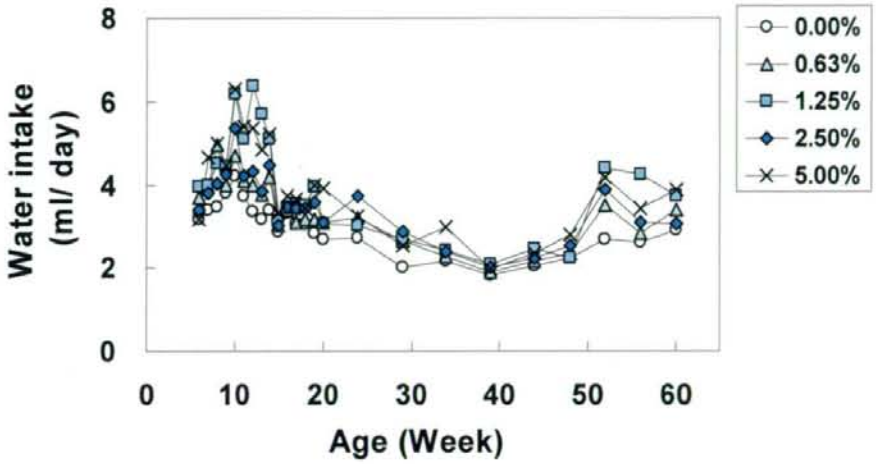

図15-2 雌*Rev1*ホモマウスの平均摂水量(ばい煎ダイズ抽出物の1年間反復投与毒性試験)

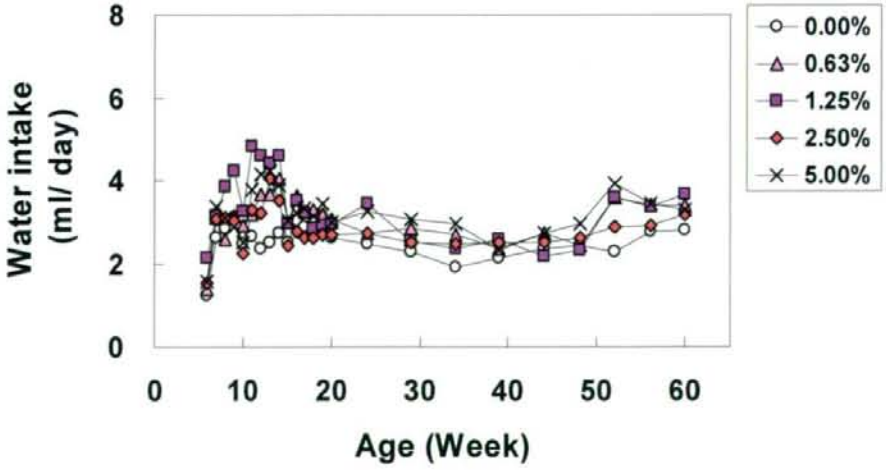

別紙4

研究成果の刊行に関する一覧表

雑誌

発表者氏名	論文タイトル名	発表誌名	巻号	ページ	出版年
Tomida, J., Masuda, Y., Hiroaki, H., Ishikawa, T., Song, I., Tsurimoto, T., Tateishi, S., Shiomi, T., Kamei, Y., Kim, J., Kamiya, K., Vaziri, C., Ohmori, H., Todo, T	DNA damage induced ubiquitylation of RFC2 subunit of RFC complex	J. Biol. Chem.	283(14)	9071-9079	2008
朴金蓮, 増田雄司, 神谷研二	ヒトREV1による損傷乗り越えDNA合成の生化学的解析	広島医学	61(4)	338-339	2008
Yoshihiko Uehara, Hironobu Ikehata, Jun-ichro Komura, Ari Ito, Masaki Ogata, Tsunetoshi Itoh, Ryoichi Hirayama, Yoshiya Furusawa, Koichi Ando, Tatjana Panuesku, Cayle E. Woloschak, Kenshi Komatsu, Shinya Matsuura, Tsuyoshi Ikura, Kenji Kamiya and Tetsuya Ono	Absence of Ku70 Gene Obliterates X-Ray-Induced lacZ Mutagenesis of Small Deletions in Mouse Tissues	Radiation Research	170(2)	216-223	2008
増田雄司, 神谷研二	誘発突然変異と損傷乗り越えDNA合成 ―REV1の構造と生化学的機能―	生化学	80(9)	843-846	2008
Gu, Y.Q., Masuda, Y., Kamiya, K	Biochemical analysis of human PIF1 helicase and functions of its N-terminal domain	Nucleic Acids Research	36(19)	6295-6308	2008

THE JOURNAL OF BIOLOGICAL CHEMISTRY VOL. 283, NO. 14, pp. 9071–9079, April 4, 2008

DNA Damage-induced Ubiquitylation of RFC2 Subunit of Replication Factor C Complex*[S]

Received for publication, December 3, 2007, and in revised form, January 18, 2008 Published, JBC Papers in Press, February 1, 2008, DOI 10.1074/jbc.M709835200

Junya Tomida[‡§], Yuji Masuda[¶], Hidekazu Hiroaki[‖], Tomoko Ishikawa[‡], Ihnyoung Song[‡‡], Toshiki Tsurimoto[§§], Satoshi Tateishi[¶¶], Tadahiro Shiomi[‖], Yasuhiro Kamei[‡**], Jinhyeong Kim[‡**], Kenji Kamiya[¶], Cyrus Vaziri[‡‡], Haruo Ohmori[§], and Takeshi Todo[‡**1]**

From the [‡]Radiation Biology Center, Kyoto University, Kyoto 606-8501, Japan, [§]Institute for Virus Research, Kyoto University, Kyoto 606-8507, Japan, [¶]Research Institute for Radiation Biology and Medicine, Hiroshima University, Hiroshima 734-8553, Japan, [‖]Division of Structural Biology, Department of Biotechnology and Molecular Biology, Graduate School of Medicine, Kobe University, Kobe 650-0017, Japan, [**]Department of Radiation Biology and Medical Genetics, Graduate School of Medicine, Osaka University, Osaka 565-0871, Japan, [‡‡]Department of Genetics and Genomics, Boston University School of Medicine, Boston, Massachusetts 02118, [§§]Department of Biology, School of Science, Kyushu University, Fukuoka 812-8581, Japan, [¶¶]Institute of Molecular Embryology and Genetics, Kumamoto University, Kumamoto 860-0811, Japan, and [‖‖]National Institute of Radiological Science, Chiba 263-8555, Japan

Many proteins involved in DNA replication and repair undergo post-translational modifications such as phosphorylation and ubiquitylation. Proliferating cell nuclear antigen (PCNA; a homotrimeric protein that encircles double-stranded DNA to function as a sliding clamp for DNA polymerases) is monoubiquitylated by the RAD6-RAD18 complex and further polyubiquitylated by the RAD5-MMS2-UBC13 complex in response to various DNA-damaging agents. PCNA mono- and polyubiquitylation activate an error-prone translesion synthesis pathway and an error-free pathway of damage avoidance, respectively. Here we show that replication factor C (RFC; a heteropentameric protein complex that loads PCNA onto DNA) was also ubiquitylated in a RAD18-dependent manner in cells treated with alkylating agents or H_2O_2. A mutant form of RFC2 with a D228A substitution (corresponding to a yeast Rfc4 mutation that reduces an interaction with replication protein A (RPA), a single-stranded DNA-binding protein) was heavily ubiquitylated in cells even in the absence of DNA damage. Furthermore RFC2 was ubiquitylated by the RAD6-RAD18 complex *in vitro*, and its modification was inhibited in the presence of RPA. The inhibitory effect of RPA on RFC2 ubiquitylation was relatively specific because RAD6-RAD18-mediated ubiquitylation of PCNA was RPA-insensitive. Our findings suggest that RPA plays a regulatory role in DNA damage responses via repression of RFC2 ubiquitylation in human cells.

Cellular DNA is continuously damaged by a vast variety of endogenous and exogenous genotoxicants. When genomic DNA is damaged, cells respond by activation of complex signaling networks that delay cell cycle progression, induce repair of lesions, activate damage tolerance pathways, and trigger apoptosis or senescence (1, 2). It is hypothesized that DNA damage-inducible signaling pathways serve important tumor-suppressive roles and prevent mutations that could lead to malignancy. Various genotoxins elicit different forms of DNA damage and result in distinct signal transduction pathways and biological outcomes. Distal steps of DNA damage-induced checkpoint signaling pathways that result in inhibition of the cell cycle are relatively well understood (3, 4). However, molecular details of proximal signaling events and lesion-specific DNA damage recognition events are less clear.

DNA replication and repair require the coordinated actions of multiple proteins on small regions of DNA. A limited number of proteins serve to coordinate multiple replication and repair events. Some proteins function commonly in DNA replication and repair and frequently have a crucial role in both processes. Three such examples are replication protein A (RPA),[2] proliferating cell nuclear antigen (PCNA), and replication factor C (RFC). RPA was originally identified as a eukaryotic single-stranded DNA-binding protein essential for *in vitro* replication of SV40 DNA (5, 6). PCNA is a trimer of three identical subunits arranged head-to-tail to generate a ringlike structure with a large central cavity for encircling DNA. It is well established that PCNA provides a mobile platform to serve as anchor and processivity factor for DNA polymerases during chromosomal replication (7, 8). PCNA is loaded onto the primer-template junction in an ATP-dependent manner by a multiprotein clamp loader, RFC (9, 10). RFC binds preferentially to double-stranded/single-stranded junctions with a recessed 3′-end, which is the DNA target for PCNA loading.

* This work was supported by grants-in-aid for Scientific Research A and B from the Ministry of Education, Culture, Sports, Science and Technology, Japan (to T. T.) and by National Institutes of Health Grants ES09558 and ES12917 (to C. V.). The costs of publication of this article were defrayed in part by the payment of page charges. This article must therefore be hereby marked "*advertisement*" in accordance with 18 U.S.C. Section 1734 solely to indicate this fact.

[S] The on-line version of this article (available at http://www.jbc.org) contains supplemental Figs. 1–5.

[1] To whom correspondence should be addressed: Dept. of Radiation Biology and Medical Genetics, Graduate School of Medicine, Osaka University, B4, 2-2 Yamada-oka, Suita, Osaka 565-0871, Japan. Fax: 81-6-6879-3819; E-mail: todo@radbio.med.osaka-u.ac.jp.

[2] The abbreviations used are: RPA, replication protein A; PCNA, proliferating cell nuclear antigen; RFC, replication factor C; Pol, polymerase; RLC, RFC-like complex; HA, hemagglutinin; PBS, phosphate-buffered saline; HU, hydroxyurea; MMS, methyl methanesulfonate; Sup, supernatant; E1, ubiquitin-activating enzyme; E2, ubiquitin carrier protein; E3, ubiquitin-protein isopeptide ligase; AP, apurinic/apyrimidinic.

RPA, PCNA, and RFC are key proteins that play central roles in DNA replication, participating in competitive polymerase switching during lagging strand synthesis. The DNA polymerase α-primase complex (Pol α) that synthesizes an RNA-DNA hybrid primer requires contact with RPA to remain stably attached to the primed site. For processive DNA synthesis to follow, Pol α must be replaced by DNA polymerase δ (Pol δ). Replacement of Pol α by Pol δ is initiated by interactions between RFC and RPA that disrupt Pol α-RPA interactions and result in removal of Pol α from DNA. After RFC loads PCNA onto the primed site, Pol δ associates with PCNA by displacing RFC. The switching process is indeed coordinated by RPA via cooperative interactions with PCNA and RFC (11, 12). RPA, RFC, and PCNA also play key roles in DNA repair by interacting with many DNA repair enzymes (13–15). Such interactions are believed to play roles in DNA damage recognition and in recruiting and positioning of DNA repair enzymes.

RFC consists of five different subunits, which are homologous to one another and are members of the AAA^+ family of ATPases (16, 17). The RFC1(p140) subunit is sometimes referred to as the "large subunit" as it contains both N- and C-terminal extensions beyond its region of homology with the four "small" subunits. The four small RFC subunits are designated RFC2(p40), RFC3(p36), RFC4(p37), and RFC5(p38) in mammals. Three protein complexes with resemblance to RFC that are involved in maintaining genome stability have been described recently. These RFC-like complexes (RLCs) share four common small subunits (RFC2–5), and each carries a unique large subunit (RAD17, CTF18, or ELG1) replacing the RFC1. These RLCs are involved in the checkpoint response (RAD17-RFC), sister chromatid cohesion (CTF18-RFC), and maintenance of genome stability (ELG1-RFC) (18, 19).

DNA damage sensors and repair proteins must react in a rapid and efficient manner to execute their functions. Frequently the regulation of these proteins involves post-translational modifications, such as phosphorylation and ubiquitylation, to help modulate the assembly and disassembly of complexes and to assist targeting and the regulation of enzymatic activity in a timely manner. For example, RPA is hyperphosphorylated upon DNA damage or replication stress by several checkpoint kinases (20). Hyperphosphorylation alters RPA-DNA and RPA-protein interactions (15, 21). Recent studies in the DNA repair field have highlighted the expanding role of ubiquitylation in the regulation of diverse DNA repair processes and pathways. One of the most striking examples of how ubiquitylation can affect protein function is that of PCNA in the budding yeast *Saccharomyces cerevisiae*. Following DNA damage, PCNA can be monoubiquitylated or polyubiquitylated on the Lys-164 residue, and each modification results in a different outcome with respect to DNA synthesis and repair (22, 23). Monoubiquitylated PCNA directs translesion synthesis via error-prone DNA polymerases, whereas polyubiquitylated PCNA is associated with an error-free DNA repair pathway (22, 23). Mammalian PCNA also undergoes monoubiquitylation after UV irradiation, and monoubiquitylated PCNA preferentially binds to translesion synthesis polymerases that contain one or two copies of ubiquitin-binding domains (24–27).

In contrast to RPA and PCNA, damage-dependent modification of RFC has not been described. Recent studies have significantly broadened the scope of the role of ubiquitylation to include regulatory functions in DNA repair and damage response pathways. Therefore, in this study we investigated whether the clamp loader RFC is likewise subjected to regulated modification. We examined the modification of all subunits in RFC and RLCs. We demonstrated that RFC2 and RFC4 are ubiquitylated following treatment of cells with alkylating agents. The ubiquitylation was partially dependent on RAD18. Surprisingly RPA inhibited the RAD18-dependent ubiquitylation of RFC2. Our results suggest that RFC regulates the DNA damage response pathway via interaction with RPA and ubiquitylation.

EXPERIMENTAL PROCEDURES

Plasmid Constructs—To generate pCDNA·RFC2(p40)FLAG and pCDNA·RFC2(p40)HA, human p40 coding region was amplified by PCR as an EcoRI-XhoI fragment. The PCR product was inserted into the EcoRI-XhoI site either of pCDNA-C-FLAG or pCDNA-C-HA. To generate pCAGGS·RFC2(p40), the human p40 coding region was amplified by PCR as a SalI-XhoI fragment. The PCR product was inserted into the XhoI site of pCAGGS. pCDNA-C-FLAG and pCDNA-C-HA was constructed by inserting the FLAG or HA epitope into the XhoI-XbaI site of pCDNA3.1. Expression plasmids containing human RFC1-FLAG, human FLAG-RAD17, human FLAG-CTF18, human FLAG-p38, human FLAG-p37, and human FLAG-p36 were constructed by inserting their cDNA described previously (28) into pCDNA3. Although N-terminally and C-terminally tagged forms of each RFC2 subunit were used, the presence of the epitope tag did not affect RFC2 regulation at least in the context of experiments reported in this study. pCAGGS·FLAG-Ubiquitin and pCAGGS·hRAD18 were constructed as described previously (25). The expression plasmids for human RFC and PCNA were described earlier (29, 30), and that for human RPA, p11d-tRPA (31), was a generous gift of Dr. Marc S. Wold (University of Iowa College of Medicine, Iowa City, IA). Mouse E1 expression vector RLC (32, 33) was a generous gift of Dr. Hideyo Yasuda (School of Life Science, Tokyo University of Pharmacy and Life Science, Tokyo, Japan). Human cDNAs for RAD6A and RAD18 amplified from a HeLa cDNA library by PCR introducing a NdeI site at the start codon were cloned together into pET20b(+) (Novagen) as an artificial operon. After cloning the PCR fragments, the nucleotide sequences were verified. All the expression plasmids of PCNA, RPA, RFC, E1, RAD6A, and RAD18 were designed for production of intact proteins without any affinity tags.

Cell Culture and Transfection—293A and HCT116 cells were grown in Dulbecco's modified Eagle's medium supplemented with 10% fetal bovine serum. HCT116 *RAD18*$^{-/-}$ cells were established as described previously (25). Cells were transfected with Lipofectamine Plus (Invitrogen) or Lipofectamine 2000 according to the manufacturer's protocol. 2.4 μg of plasmid DNA was used to transfect each 6-cm plate of cells. Transfected cells were treated with genotoxins 24 h post-transfection.

Genotoxin and Inhibitor Treatments—Asynchronous cell cultures were grown to approximately 80% confluency. For UV

treatment, cells were washed with PBS, and exposed to UV light (254 nm) at a fluence rate of 43 J m^{-2}/s. For genotoxin and inhibitor treatment, hydroxyurea (HU; 1 M in H_2O), aphidicolin (dissolved in Me_2SO), methyl methanesulfonate (MMS; dissolved in Me_2SO), ethyl methanesulfonate (dissolved in Me_2SO), *N*-methyl-*N'*-nitro-*N*-nitrosoguanidine (dissolved in Me_2SO), H_2O_2 (diluted in PBS), mitomycin C, bleomycin (dissolved in H_2O), or camptothecin (dissolved in Me_2SO) was added to the culture media to give a final concentration of 2 mM, 0.025 mM, 0.1–1.7 mM, 20 mM, 0.7 mM, 0.5 mM, 0.01 mM, 0.05 mg/ml, or 20 nM, respectively, and cells were exposed for 8 h unless otherwise stated.

Antibodies—A mouse monoclonal antibody against *Drosophila* RFC40 (anti-dRFC40) was used for probing human RFC2(p40). A hybridoma cell line producing anti-dRFC40 antibody was a kind gift from Dr. Gerald M. Rubin (University of California, Berkeley), and monoclonal antibody was purified as described previously (34). To test whether anti-dRFC40 antibody cross-reacts with human RFC2(p40), an HA epitope-tagged form of hRFC2(p40) was overexpressed in 293A cells by transfection, and cell lysate was recovered 24 h post-transfection and then immunoblotted with either anti-dRFC40 or anti-HA antibody. An anti-dRFC40-reactive protein band migrating at 40 kDa was clearly observed only in extracts from HA-hRFC2(p40)-transfected cells and corresponded to the species detected with an anti-HA antibody (supplemental Fig. 1). Therefore, the anti-dRFC40 antibody recognizes human RFC2(p40). To avoid confusion we refer to the anti-dRFC40 antibody as "anti-RFC2" antibody in this study.

Other commercial antibodies used in this study were: anti-HA (Y-11, Santa Cruz Biotechnology), anti-FLAG (M2, Sigma), anti-RFC1 (H-300, Santa Cruz Biotechnology), anti-RAD17 (H-3, Santa Cruz Biotechnology), anti-tubulin (B-5-1-2, Sigma), anti-histone H3 (6.6.2, Upstate; and ab1791, Abcam), and anti-PCNA (PC10, Oncogene).

Preparation of Cell Lysate and Chromatin Fraction—293A cells in a 3.5- or 6-cm dish were washed twice with ice-cold PBS and then harvested into radioimmune precipitation assay buffer (1× PBS, 1% Nonidet P-40, 0.5% sodium deoxycholate, 0.1% SDS, 1 mM phenylmethylsulfonyl fluoride, 1 mM sodium orthovanadate, and protease inhibitor (Nacalai)). The cell suspensions were incubated for 30 min on ice, and then the Nonidet P-40, 0.1% SDS-insoluble fraction and -soluble fractions were separated by centrifugation. The soluble fraction was used as the supernatant (Sup) fraction. The resultant pellet was washed with radioimmune precipitation assay buffer four times and then sonicated after adding SDS-PAGE loading buffer (7% glycerol, 22% SDS, 50 mM Tris-HCl (pH 6.8), 5% β-mercaptoethanol). The resultant solution was used as the chromatin fraction. We confirmed that there were few contaminations in each Sup and chromatin fraction using anti-tubulin and anti-histone H3 antibodies (supplemental Fig. 2).

SDS-PAGE and Western Blotting—Cell extracts were resolved by electrophoresis by 7.5 or 10% SDS-PAGE. Following transfer onto polyvinylidene difluoride or nitrocellulose filters, the blots were incubated with antibodies, and immunoblots were visualized by enhanced chemiluminescence (ECL, Amersham Biosciences; or DURA, Pierce) according to the manufacturers' instructions.

Immunoprecipitation—Cell extracts were incubated with monoclonal mouse anti-RFC2 (dRFC4(p40)) antibody for 1 h at 4 °C and then with 25 μl of protein A/G-agarose (Santa Cruz Biotechnology). After incubation for overnight at 4 °C, the beads were washed with PBS three times and boiled in Laemmli buffer for 5 min, and the bound proteins were analyzed by electrophoresis and immunoblotting.

Protein Purification—Human RFC, PCNA, and RPA were purified as described previously (29, 30). Mouse E1 was overproduced in insect cells and purified as described previously (35). Human RAD6A-RAD18 complex was overproduced in *Escherichia coli* cells and then purified by column chromatography (phosphocellulose, heparin-Sepharose, Mono Q, and gel filtration) from *E. coli* cell lysate. Protein concentrations were determined by Bio-Rad protein assay kit using bovine serum albumin as the standard. Bovine ubiquitin was purchased from Sigma.

In Vitro Ubiquitylation Assay—The reaction mixture (25 μl) contained 20 mM HEPES-NaOH (pH 7.5), 50 mM NaCl, 0.2 mg/ml bovine serum albumin, 1 mM dithiothreitol, 10 mM $MgCl_2$, 1 mM ATP, 33 fmol of singly primed single-stranded M13 mp18 DNA (30), 1.0 μg (9.1 pmol) of RPA, 86 ng (1.0 pmol as a trimer) of PCNA, 75 ng (260 fmol) of RFC, 100 ng (850 fmol) of mouse E1, 175 ng (2.4 pmol) of RAD6A-RAD18 complex, and 12.5 μg (1460 pmol) of ubiquitin. After incubation at 30 °C for 60 min, reactions were terminated with 2 μl of 300 mM EDTA.

Structural Model Building—Homology modeling of the human clamp loader-clamp complex was performed using MODELLER version 7.7 (36). The homologous structures were defined using the fold recognition server FORTE (37). The atomic coordinate of the clamp-clamp loader complex (Protein Data Bank code 1SXJ) was selected as a template for model building. Before submission to MODELLER, the sequence-structure alignment obtained from FORTE was used. Due to the lack of the template structure, the N-terminal 582 residues of human RFC1 were not modeled. The figures were prepared using MOLMOL (38). Coloring of each RFC subunit and PCNA was according to Fig. 2 in the review by Bowman *et al.* (39).

RESULTS

Specific DNA-damaging Agents Induce Modification of RFC2—To analyze the modification of each subunit of the RFC complex, a FLAG epitope-tagged form of each subunit of RFC and RLCs was expressed in human 293A cells. Transfected cells were treated with UV irradiation, γ-ray, HU, or MMS, and then cell extracts were prepared. The cell extracts were separated into Nonidet P-40-insoluble chromatin fractions and -soluble fractions (Sup). RFC and RLC subunits in each fraction were analyzed by SDS-PAGE and Western blotting (Fig. 1*A*). Following MMS treatment all of the subunits, except for CTF18 and RFC5, accumulated in the chromatin fraction, whereas no accumulation was observed following treatments with UV irradiation, γ-ray, or HU. Levels of soluble CTF18 and RFC5 decreased after MMS treatment, although we did not detect concomitant increases in the chromatin-bound levels of these

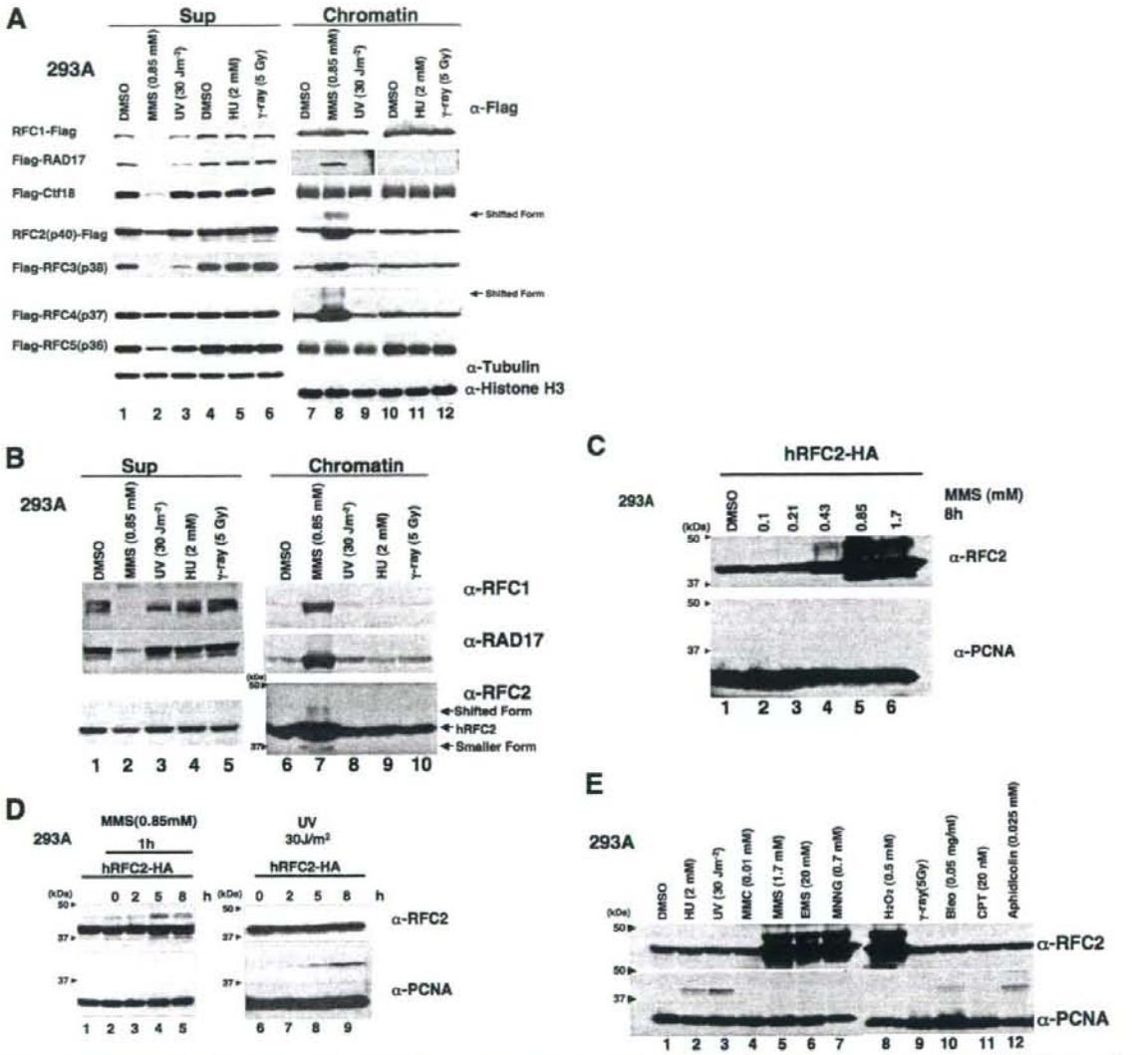

FIGURE 1. **Accumulation of RFC complex in chromatin fraction and modification of RFC2 following treatment of 293A cells with DNA-damaging agents.** *A*, 293A cells transfected with a FLAG epitope-tagged form of each subunit of RFC and RLCs were irradiated with UV light (*lanes 3* and *9*) or γ-ray (*lanes 6* and *12*) or treated with Me_2SO (*DMSO*; *lanes 1*, *4*, *7*, and *10*), MMS (*lanes 2* and *8*), or HU (*lanes 5* and *11*) for 8 h. Cell extracts recovered from transfected cells were then separated into chromatin (*lanes 7–12*) and soluble (*Sup*; *lanes 1–6*) fractions and analyzed by Western blotting with anti-FLAG. Cell extracts recovered from RFC4-transfected cells were also analyzed by Western blotting with anti-tubulin or anti-histone H3 (*lowest two blots*). *B*, 293A cells were irradiated with UV light (*lane 3*) or γ-ray (*lane 5*) or treated with Me_2SO (*lane 1*), MMS (*lane 2*), or HU (*lane 4*) for 8 h. Cell extracts recovered from transfected cells were then separated into chromatin and soluble (*Sup*) fractions and analyzed by Western blotting either with anti-RFC1, anti-RAD17, or anti-RFC2. The *arrowheads* indicate the position of molecular mass markers (kDa). *C*, 293A cells transfected with pCDNA3-RFC2-HA were treated with the indicated dose of MMS for 8 h. Chromatin fractions from the resulting cells were analyzed by immunoblotting with anti-RFC2 or anti-PCNA. The *arrowheads* indicate the position of molecular mass markers (kDa). *D*, 293A cells transfected with pCDNA3-RFC2-HA were treated with 0.85 mM MMS for 1 h (*lanes 2–5*) or UV light-irradiated at 254 nm with 30 J m^{-2} (*lanes 6–9*) and then incubated for the indicated times. Chromatin fractions were prepared and analyzed by Western blotting with anti-RFC2 and anti-PCNA. Cells treated with Me_2SO (*lane 1*) are shown as control. The *arrowheads* indicate the position of molecular mass markers (kDa). *E*, 293A cells transfected with pCDNA3-RFC2-HA were treated with various genotoxic agents. Chromatin fractions were prepared and analyzed by Western blotting with anti-RFC2 or anti-PCNA. The *arrowheads* indicate the position of molecular mass markers (kDa). *Gy*, grays; *MMC*, mitomycin C; *EMS*, ethyl methanesulfonate; *MNNG*, *N*-methyl-*N'*-nitro-*N*-nitrosoguanidine; *Bleo*, bleomycin; *CPT*, camptothecin.

subunits (Fig. 1*A*). Taken together, the results of Fig. 1*A* demonstrate that the levels and subcellular distribution of RFC and RLC subunits are regulated in response to MMS.

It was important to determine whether endogenous RFC and RLC subunits were also redistributed to chromatin in response to MMS. Therefore, we determined the effects of MMS on endogenous RFC1, RAD17, or RFC2 proteins for which good antibodies are available. As shown in Fig. 1*B*, endogenous RFC1, RAD17, and RFC2 accumulated in the chromatin fraction of MMS-treated 293A cells. Similar to

ectopically expressed tagged proteins, endogenous RFC subunits were redistributed to chromatin in response to MMS treatment.

Interestingly we observed prominent forms of ectopically expressed RFC2 and RFC4 that migrated with reduced electrophoretic mobility on SDS-PAGE gels in chromatin fractions from MMS-treated 293A cells (Fig. 1*A*, *lane 7*). Electrophoretically retarded species of endogenous RFC2 were also evident in chromatin fractions of MMS-treated 293A cells (Fig. 1*B*, *lane 7*). The electrophoretically shifted form of RFC2 was more prominent than that of RFC4 (Fig. 1*A*). Therefore we focused on RFC2 and further analyzed its MMS-induced modification.

We performed quantitative analyses to determine the amount of chromatin-bound RFC2 relative to the soluble fraction in MMS-treated cells. In 293A cells ectopically expressing HA-tagged RFC2, more than 90% of the RFC2 accumulated in the chromatin fraction following 8 h of MMS treatment, whereas in untreated cells, less than 10% of RFC2 was present in the chromatin fraction (supplemental Fig. 3). Following MMS treatment, we consistently detected two electrophoretically retarded anti-RFC2-reactive proteins in the chromatin fraction. The apparent molecular mass of electrophoretically retarded RFC2 is consistent with ubiquitylation. The two putative ubiquitylated forms of RFC2 (shown in Fig. 1) might correspond to species that are monoubiquitylated on different residues. However, we cannot exclude the possibility that modifications other than ubiquitin are also present on the shifted RFC2. Furthermore smaller anti-RFC2-reactive proteins, possibly corresponding to degradation products, were detected in soluble and chromatin fractions from both control and MMS-treated cells (Fig. 1*B* and supplemental Fig. 3).

The electrophoretically retarded forms of RFC2 were induced by MMS in a dose-dependent manner (Fig. 1*C*). At lower concentrations of MMS (0.1 or 0.213 mM), no RFC2 band shift was detectable. However, treatment with higher concentrations of MMS (0.425, 0.85, or 1.7 mM) induced prominent electrophoretically retarded forms of RFC2 on chromatin (Fig. 1*C*).

In the experiments described above, the cells were treated with MMS for 8 h. We subsequently examined the kinetics of RFC2 modification by treating 293A cells with MMS (0.85 mM) for 1 h and preparing samples for immunoblotting at 0, 2, 5, and 8 h following MMS treatment. As shown in Fig. 1*D*, the shifted forms of RFC2 were detectable by 5 h after treatment of cells with MMS (*lane 4*). Similar to results of Fig. 1*A*, the genotoxin-induced RFC2 mobility shift was specific for MMS because UV irradiation (30 J/m^2; *lanes 7–9*) did not induce RFC modification at any time point tested (although as expected, UV irradiation induced PCNA monoubiquitylation under these experimental conditions). Conversely little or no PCNA modification was detectable under the conditions used for the experiment shown in Fig. 1*D* (*lanes 2–5*), although low levels of PCNA ubiquitylation were observed when cells were treated with 0.85 mM MMS for longer times (data not shown).

The results of Fig. 1, *A* and *D*, indicated that MMS-induced RFC2 modification is not a general response to DNA damage. To gain insight into the significance of RFC2 modification, 293A cells ectopically expressing RFC2-HA were treated with a more extensive panel of DNA-damaging agents for 8 h, and proteins in resulting chromatin fractions were analyzed by immunoblotting with the anti-RFC2 antibody (Fig. 1*E*, *upper panel*). DNA-damaging agents we tested included alkylating agents (ethyl methanesulfonate and *N*-methyl-*N*′-nitro-*N*-nitrosoguanidine), an oxidizing agent (H_2O_2), a DNA cross-linking agent (mitomycin C), double strand break-inducing agents (bleomycin and ionizing radiation), and the topoisomerase I inhibitor camptothecin. Of the genotoxic agents tested, only ethyl methanesulfonate, *N*-methyl-*N*′-nitro-*N*-nitrosoguanidine, and H_2O_2 induced the shifted RFC2 band evident in MMS-treated cells (Fig. 1*E*, *upper panel*, *lanes 7–10*). Many of the agents failing to induce the RFC2 band shift nevertheless induced very robust PCNA monoubiquitylation (Fig. 1*E*, *lower panel*). Therefore, we conclude that RFC2 modification is a specific response to a subset of genotoxins.

RAD18-dependent Ubiquitylation of Human RFC2—To test whether the shifted RFC2-specific band in MMS-treated cells was due to ubiquitylation, RFC2-HA was co-expressed with FLAG-tagged ubiquitin in 293A cells. The transfected cells were treated with MMS. Endogenous and HA-tagged RFC2 proteins were immunoprecipitated with anti-RFC2 antibody from cell lysates, and the precipitated proteins were immunoblotted with either anti-RFC2 (Fig. 2*A*, *upper panel*) or anti-FLAG antibody to detect FLAG-ubiquitin-modified proteins (*lower panel*). Anti-RFC2-reactive bands migrating at the sizes expected for monoubiquitylated RFC2 (48 kDa) were observed in our anti-RFC2 immunoprecipitates (*lanes 3* and *4*, *Ub-RFC2*). In addition to the 48-kDa ubiquitin-RFC2 band, two extra, slowly migrating bands (51 and 62 kDa) were observed in the immunoprecipitates obtained from cells transfected with FLAG-tagged ubiquitin (*lane 4*, *Flag-Ub-RFC2*) that were also detectable by immunoblotting with anti-FLAG antibody (*lane 8*). From these results we conclude that the slow migrating forms of RFC2 in MMS-treated cells are ubiquitylated species.

In *S. cerevisiae* and human cells, monoubiquitylation of PCNA is dependent on the RAD18 E3 ubiquitin ligase (22, 24, 25). To determine whether ubiquitylation of RFC2 was similarly dependent on RAD18, RFC2 modification was tested in RAD18-overexpressing 293A cells (Fig. 2*B*) and *RAD18*-deficient HCT116 cells (Fig. 2*C*). As shown in Fig. 2*B*, overexpression of RAD18 induced the ubiquitylation of RFC2-HA and PCNA even in the absence of MMS treatment. Conversely MMS-induced ubiquitylated forms of RFC2 decreased considerably (by 50%) in HCT116 *RAD18*$^{-/-}$ cells compared with those in matched HCT116 *RAD18*$^{+/+}$ cells (Fig. 2*C*). These results suggest that RFC2 monoubiquitylation in MMS-treated cells is mediated at least in large part by RAD18, most probably as a complex with RAD6. Interestingly RAD18 overexpression also induced chromatin accumulation of RFC2 (Fig. 2*B*). Ubiquitylation and chromatin accumulation of RFC2 (and also RFC4) was observed in response to MMS treatment and RAD18 overexpression. Because MMS treatment induced chromatin accumulation of each RFC subunit (Fig. 1*A*), it is most likely that increased chromatin loading of the entire RFC complex occurs in response to MMS.

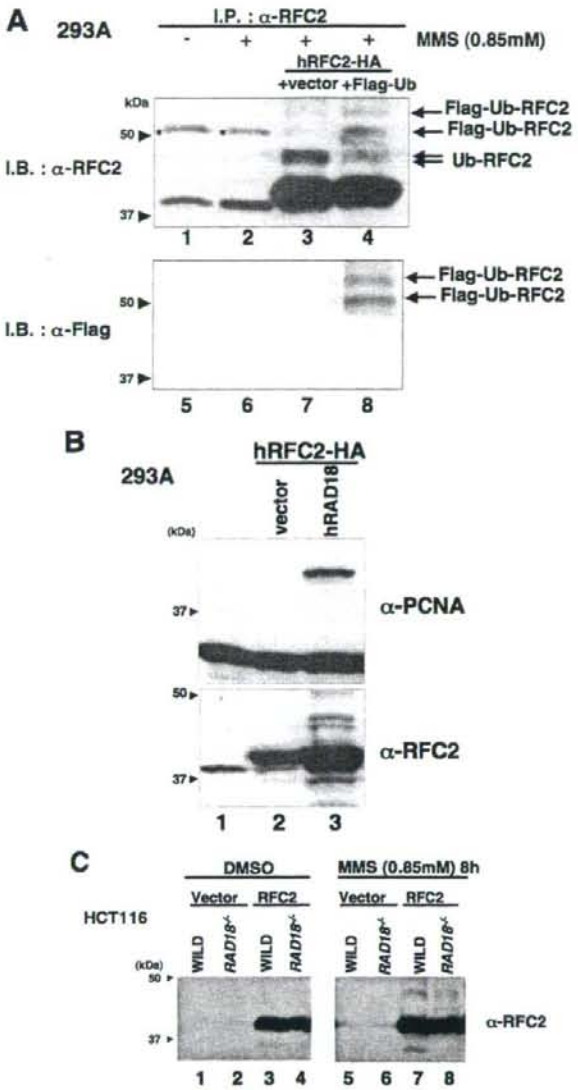

FIGURE 2. **RFC2 monoubiquitylation in response to DNA-damaging agents is RAD18-dependent.** *A*, lysates from RFC2-HA- and FLAG-ubiquitin-co-transfected 293A cells were analyzed by immunoprecipitation and Western blotting. pCDNA3-RFC2-HA was co-transfected either with pCAGGS-FLAG-Ubiquitin (*lanes 4* and *8*) or empty vector (*lanes 3* and *7*) in 293A cells. The following day, cells were treated with MMS for 8 h, and then cell extracts were recovered. Cell extracts were immunoprecipitated with anti-RFC2 antibody. The resulting immune complexes were recovered using protein A/G-agarose and detected by immunoblotting with anti-RFC2 antibody (*lanes 1–4*) or anti-FLAG antibody (*lanes 5–8*). *Asterisks* show nonspecific bands. *B*, Western blot of lysates from 293A cells overexpressing hRAD18. pCDNA3-RFC2-HA was co-transfected either with pCAGGS-hRAD18 (*lane 3*) or empty vector (*lane 2*) in 293A cells. Chromatin fractions were prepared and analyzed by Western blotting with anti-RFC2 (*lower panel*) or anti-PCNA (*upper panel*). The *arrowheads* indicate the position of molecular mass markers (kDa). *C*, Western blot of lysates from HCT116 cells (*WILD*) or *RAD18*-deficient HCT116 cells (*RAD18*$^{-/-}$). HCT116 cells transfected either with empty vector or pCAGGS-hRFC2 were treated with 0.85 mM MMS for 8 h. Chromatin fractions from the resulting cells were analyzed by immunoblotting with anti-RFC2 antibody. The *arrowheads* indicate the position of molecular mass markers (kDa). *I.P.*, immunoprecipitate; *I.B.*, immunoblot; *DMSO*, Me_2SO; *Ub*, ubiquitin.

An RFC2 Mutant Is Ubiquitylated in the Absence of DNA Damage—It has been reported that the RFC2(p40) subunit of human RFC binds the large subunit of RPA (11). In *S. cerevisiae*, a mutation in *rfc4* (yeast homolog of human RFC2(p40)) was found to display synthetic lethality with mutation in the gene encoding Rpa1 (the large subunit of *S. cerevisiae* RPA) (40). Interestingly this mutant Rfc4(p40) showed weaker physical interaction with RPA than did the wild type Rfc4(p40). This mutation, resulting in an amino acid change of aspartate to asparagine at residue 201, maps to the RFC box VIII, which is one of the conserved motifs found in all RFC subunits (16, 41). The Asp-201 residue of *S. cerevisiae* Rfc4 is conserved and found at an identical position in RFC2 from higher eukaryotes, including humans (Fig. 3*A*). We replaced Asp-228 of human RFC2 (which corresponds to *S. cerevisiae* Rfc4 Asp-201) with an asparagine residue (D228N) or an alanine (D228A). HA-tagged forms of mutant or wild-type RFC2 were expressed in 293A cells by transfection (Fig. 3*B*). The wild-type and mutant forms of RFC2-HA were expressed at similar levels; however, whereas the wild-type and D228N mutant RFC2 proteins showed no ubiquitylation of RFC2, the D228A mutant RFC2 protein underwent extensive modification without any genotoxin treatment (Fig. 3*B*, *lane 8*). The multiple shifted bands of RFC2 D228A decreased by 55% in HCT116 *RAD18*$^{-/-}$ cells compared with those in matched HCT116 *RAD18*$^{+/+}$ cells (Fig. 3*C*). Therefore, we conclude that the multiple RAD18-dependent species we observed correspond to mono- and polyubiquitylated forms of RFC2. As described in the previous sections, we observed monoubiquitylated forms of the wild-type RFC2-HA in MMS-treated cells but did not observe high levels of its polyubiquitylated forms. The results of Fig. 3*B* indicate that the RFC2 D228A mutant is extensively ubiquitylated and accumulates as multiple polyubiquitylated species (even in the absence of genotoxin treatments) when ectopically expressed. Although the difference in susceptibility to spontaneous ubiquitylation between D228A and D228N is unexpected, by analogy with the *S. cerevisiae* Rfc4 D201N mutant protein, it is most likely that Asp-228 of human RFC2 is also involved in interaction with RPA. Although we have not formally verified the reduced interaction of human RFC D228A with RPA, we infer that RAD6-RAD18-mediated RFC2 ubiquitylation is regulated by interaction with RPA (see below).

RFC2 Is Modified by the RAD6-RAD18 Complex in Vitro—We subsequently examined whether RFC2 could be modified by the RAD6-RAD18 complex *in vitro*. Recombinant RFC complex (including RFC1–5 proteins of human origin) was expressed in *E. coli* and then purified. Monoubiquitylation of RFC2 *in vitro* was investigated by mixing the RFC1–5 complex with purified recombinant RAD6A (E2 ubiquitin-conjugating enzyme)-RAD18 (E3 ubiquitin ligase) complex. As shown in Fig. 4, RFC2 was monoubiquitylated *in vitro* when incubated in the presence of purified RAD6A and RAD18 plus ubiquitin and its activating enzyme (*lane 2*) although at a much lower efficiency when compared with PCNA. It should also be noted that the *in vitro* modification of RFC2 generated only a single monoubiquitylated species, whereas at least two monoubiquitylated forms of RFC2 (corresponding to monoubiquitylation at

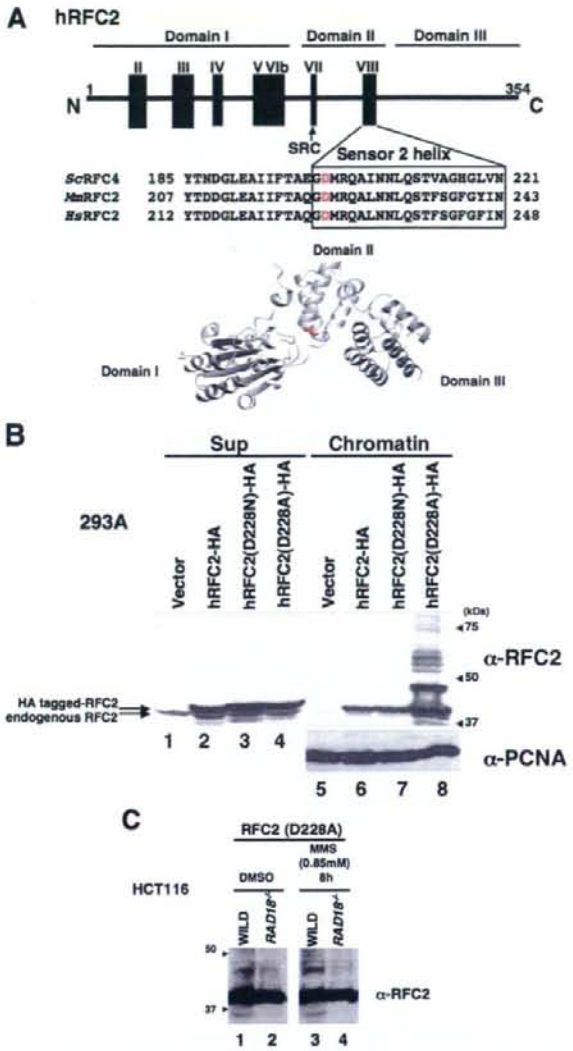

FIGURE 3. **DNA damage-independent monoubiquitylation of hRFC2 D228A.** *A*, schematic diagram and tertiary model of human (*Hs*) RFC2 showing the location of Asp-228 and the sequences of the surrounding regions. Corresponding sequences for *S. cerevisiae* (*Sc*) RFC2(p40) and mouse (*Mm*) RFC2 homologues are also shown. The conserved Sensor 2 helix is represented by a *box*, and the location of the conserved SRC motif is indicated by an *arrow*. Asp-228 of hRFC2, shown in *red*, corresponds to *S. cerevisiae* Asp-201, which shows synthetic lethality with mutation in Rpa-1(*rfa1*-Y29H). There are seven conserved RFC boxes *numbered* consecutively from the N terminus to C terminus. *B*, 293A cells were transfected with expression vectors encoding wild-type (*lanes 2* and *6*), D228N (*lanes 3* and *7*), or D228A (*lanes 4* and *8*) forms of hRFC2-HA. 24 h after transfection cells were harvested and separated into chromatin (*lanes 5–8*) and soluble fractions (*lanes 1–4*) and then immunoblotted with anti-RFC2 or anti-PCNA antibody. The *arrowheads* indicate the position of molecular mass markers (kDa). *C*, Western blot of lysates from HCT116 cells (*WILD*) or *RAD18*-deficient HCT116 cells (*RAD18*$^{-/-}$). HCT116 cells transfected with pCAGGS-hRFC2(Asp-228) were treated with 0.85 mM MMS for 8 h. Chromatin fractions from the resulting cells were analyzed by Western blotting with anti-RFC2 antibody. The *arrowheads* indicate the position of molecular mass markers (kDa). *DMSO*, Me_2SO.

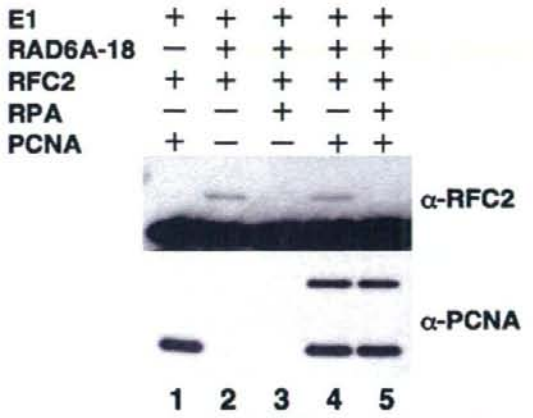

FIGURE 4. ***In vitro* monoubiquitylation of RFC2.** *In vitro* ubiquitylation was carried out by mixing RFC with mouse E1, RAD18-RAD6A complex, ubiquitin, and singly primed single stranded M13 mp18 DNA in the presence or absence of RPA or PCNA as indicated. The reaction products were analyzed by Western blotting with anti-RFC2 or anti-PCNA antibody.

different residues) resulted from MMS treatment of intact cells. The reason for the differential patterns of RAD18-mediated RFC2 monoubiquitylation observed *in vitro* and in intact cells is not yet clear but could result from the existence of additional RFC2-directed E3 ligases *in vivo*. The difference also indicates that *in vitro* assay conditions do not fully recapitulate the complexity of events involved in RPA-sensitive RFC2 ubiquitylation at stalled replication forks *in vivo*. It should be noted that our *in vitro* assay uses primed M13 single-stranded DNA, which mimics the leading strand synthesis rather than the lagging strand synthesis that requires the RFC complex more frequently. PCNA did not affect RFC2 monoubiquitylation (*lane 4*), although the modification was dependent on the presence of DNA (data not shown). Interestingly, however, the addition of RPA inhibited RAD6-RAD18-dependent monoubiquitylation completely (*lanes 3* and *5*). In parallel reactions, RPA did not affect the monoubiquitylation of PCNA (*lanes 4* and *5*). Therefore, RPA specifically inhibits RAD18-dependent monoubiquitylation of RFC2. The inhibition of RAD18-mediated RFC2 ubiquitylation by RPA *in vitro* is consistent with our finding that the RFC2 D228A mutant is more extensively modified than wild-type RFC2 in intact cells.

DISCUSSION

Protein ubiquitylation is critical for numerous cellular functions, including the DNA damage response pathway. In this study we demonstrated that RFC2 is ubiquitylated in human cells via DNA damage-independent and genotoxin-inducible mechanisms. RFC2 ubiquitylation is partially dependent on RAD18 as demonstrated by the decreased MMS-induced RFC2 ubiquitylation in *RAD18*$^{-/-}$ cells compared with matched *RAD18*$^{+/+}$ HCT116 cells (Fig. 2*C*). Conversely RFC2 undergoes genotoxin-independent monoubiquitylation in cells overexpressing RAD18. RAD18-dependent monoubiquitylation of RFC2 was also verified by *in vitro* reaction (Fig. 4). The RAD18-induced ubiquitylation of RFC2 *in vitro* and in RAD18-overexpressing cultured cells is similar to what we and others have

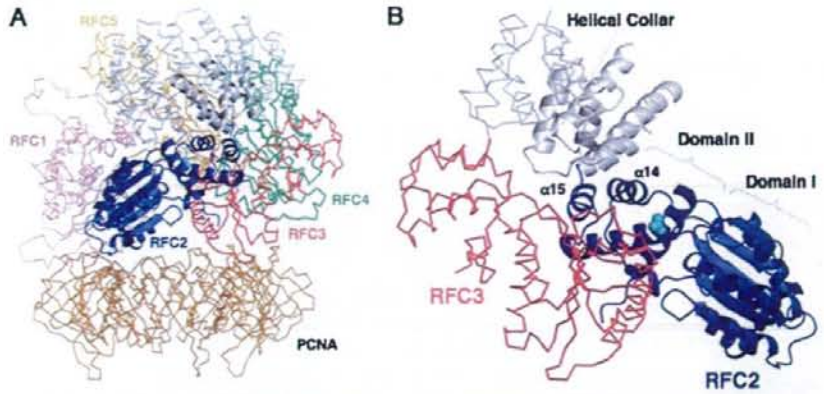

FIGURE 5. **A model for human clamp loader-clamp complex.** Ribbon (RFC2) and wire (Cα trace, RFC1, RFC3–5, and PCNA) representations of the homology model for human RFC1–5-PCNA complex are shown. The five subunits of each clamp loader complex are denoted. The colors for each of the subunits are as follows with the helical collar domains (*gray*) at the top of the figure: *pink*, RFC1; *navy*, RFC2; *red*, RFC3; *green*, RFC4; *orange*, RFC5; *gold*, PCNA. The side chain atoms of Asp-228 of RFC2 are indicated as *balls* in *cyan*. *A*, a side view of the clamp loader-clamp complex in which RFC2 is in the front. *B*, views from the DNA-interacting pore of the clamp loader subunits. Domains I and II of AAA$^+$ domain and α14 and α15 of RFC2 are indicated.

observed for PCNA, a *bona fide* RAD18 substrate. These results are further indicative of a direct E3 ligase-substrate relationship between RAD18 and RFC2.

Our *in vitro* experiments clearly show an inhibitory effect of RPA on RFC2 monoubiquitylation (Fig. 4). The involvement of RPA in regulation of RFC2 ubiquitylation *in vivo* is also suggested by our experiments with the RFC2 D228A mutant (corresponding to an *S. cerevisiae* RPA interaction-deficient Rfc4 mutant). We have shown that RFC2 D228A underwent DNA damage-independent ubiquitylation, which was reduced substantially in RAD18-deficient cells (Fig. 3*C*). Our *in vitro* assay for RAD6-RAD18-dependent RFC2 ubiquitylation did not completely recapitulate all aspects of RFC2 modification *in vivo*, and the role of RFC2 D228 in mediating RPA associations is not yet clear. However, our results strongly suggest a key regulatory role of RPA in RFC2 ubiquitylation. We propose that RAD18-dependent RFC2 ubiquitylation is repressed by RPA in undamaged cells and that derepression of RFC2 ubiquitylation occurs following MMS-induced DNA damage.

Our experiments also indicate that the RFC2 D228A mutant is subject to extensive polyubiquitylation. It is likely that polyubiquitylated RFC2 is generated by linkage of additional ubiquitin molecules to lysine residues that are first monoubiquitylated by RAD18. By analogy, following genotoxin treatments PCNA is monoubiquitylated by RAD6-RAD18 on lysine 164, and subsequently the monoubiquitylated PCNA is polyubiquitylated in a reaction mediated by MMS2-UBC13 and RAD5 (22, 23, 42, 43). It will be interesting to determine whether RAD5 or alternative E3 ligases contribute to the RAD18-initiated polyubiquitylation of RFC2. Monoubiquitylated and polyubiquitylated species of PCNA promote different damage response pathways, error-prone and error-free postreplication repair, respectively. It will be interesting to determine whether the mono- and polyubiquitylated species of RFC2 similarly serve distinct effector functions. Several studies have demonstrated that a residual level of PCNA ubiquitylation is detectable in RAD18-deficient cells. Similarly we have shown that RAD18-deficiency did not completely ablate RFC2 ubiquitylation. Clearly further work is necessary to identify the E3 ligases involved in RAD18-independent ubiquitylation of PCNA and RFC2.

To obtain insight into the question of why the RFC2 D228A mutant is susceptible to ubiquitylation without DNA damage, we constructed tertiary structure models of human RFC2 (Fig. 3*A*) and RFC complex bound to PCNA (Fig. 5) by homology modeling using the reported yeast structure (41) as the template. Each RFC subunit contains three structurally conserved domains (Domains I, II, and III). Domains I and II comprise an ATPase module of the AAA$^+$ family that is connected by a flexible linker to another helical domain (Domain III). Our structural model revealed that Asp-228 resides in the turn between helix14 and helix15 (Sensor 2 helix), which is located near the hinge region between Domains II and III (Fig. 5*C*). This implies that RFC2 Asp-228 is not exposed to the outer surface but instead is buried in the spiral structure. It is unlikely, therefore, that the Asp-228 residue directly associates with RPA as long as such a tight RFC-PCNA complex is maintained.

Whether the RFC complex remains around the primed end following PCNA loading is controversial (11, 30, 44–46). However, the RFC complex may stay associated with PCNA in a structure different from the tight complex as shown in Fig. 5*A* that allows RPA to associate with RFC2 around the Asp-228 residue. Another possibility is that the D228A mutation causes a conformational change in the RFC complex structure, possibly altering interactions with RPA and affecting susceptibility to ubiquitylation.

It is notable that RFC2 is ubiquitylated in human cells following treatment with alkylating agents but not in response to genotoxins that induce double strand breaks, bulky adducts, interstrand cross-links, or nucleotide depletion. Therefore, it appears that RFC2 monoubiquitylation is due to a specific alteration in DNA structure induced by alkylating agents or to a specific DNA repair intermediate. Identification of the DNA structure(s) responsible for RFC2 ubiquitylation may provide insight into the consequences of DNA damage due to particular genotoxins. Alkylating agents modify DNA by adding methyl or ethyl groups to a number of nucleophilic sites on the DNA bases (47). The predominant adduct in double strand DNA resulting from MMS or *N*-methyl-*N*′-nitro-*N*-nitrosoguanidine exposure is N^7-methylguanine (N^7-MeG) and N^3-methyladenine (N^3-MeA). N^3-MeA blocks replication, whereas N^7-MeG does not block replication or miscode. Another deleterious adduct is O^6-methylguanine (O^6-MeG). O^6-MeG is produced at a relatively lower level compared with N^7-MeG and N^3-MeA but is highly mutagenic and toxic because O^6-MeG-T mispairing not only results in G/C to A/T transition but also is

recognized by mismatch repair in a process that is a potent signal of apoptosis (48). However, the human kidney cell line 293A cells, which were used in this study, are mismatch repair-deficient due to epigenetic silencing of the *hMLH1* gene by promoter hypermethylation (49). Therefore, O^6-MeG is not the lesion responsible for RFC2 monoubiquitylation, and instead N^7-MeG and/or N^3-MeA are the likely candidates. Treatment of 293A cells with an oxidative agent (H_2O_2) also induced RFC2 monoubiquitylation (Fig. 1*E*). Base excision repair is the common pathway for repairing N^7-MeG, N^3-MeA, and oxidative damage (47, 50, 51). Base excision repair is initiated with removal of altered bases by DNA glycosylase. The resulting apurinic/apyrimidinic (AP) sites are nicked, and repair is completed by resynthesis and ligation. Therefore, for proficient base excision repair, a proper balance of the individual steps involved in DNA repair is important. Imbalanced base excision repair may result in deleterious intermediates, such as AP sites. Furthermore methylation or oxidation of purines destabilizes the *N*-glycosyl bond, thus rendering the base more susceptible to hydrolysis to form an AP site. Therefore, AP sites are the lesions most likely to cause RFC2 monoubiquitylation, although precisely how RPA-RFC2 interaction is affected at AP sites is unclear.

Another possible role of RFC2 ubiquitylation is as the sensing signal for damage recognition. The RFC1–5 complex (containing RFC2) has several functions. During normal DNA replication RFC1–5 acts as clamp loader for PCNA, whereas in the DNA damage response RAD17-RFC2–5 loads the 9-1-1 complex. At present we do not know whether loading of PCNA, the 9-1-1 complex, or both is affected by RAD18-dependent RFC2 modification. Experiments to further address the significance of RFC2 modification and to identify relevant effectors of modified RFC are under way.

Acknowledgments—We greatly appreciate the gift of the expression plasmids for human RPA, p11d-tRPA, from Dr. Marc S. Wold (University of Iowa College of Medicine, Iowa City, IA) and mouse E1 expression vector RLC from Dr. Hideyo Yasuda (School of Life Science, Tokyo University of Pharmacy and Life Science, Tokyo, Japan).

REFERENCES

1. Hartwell, L. H., and Weinert, T. A. (1989) *Science* **246,** 629–634
2. Carr, A. M. (2002) *DNA Repair (Amst.)* **1,** 983–994
3. Kastan, M. B., and Bartek, J. (2004) *Nature* **432,** 316–323
4. Sancar, A., Lindsey-Boltz, L. A., Unsal-Kacmaz, K., and Linn, S. (2004) *Annu. Rev. Biochem.* **73,** 39–85
5. Bochkareva, E., Korolev, S., Lees-Miller, S. P., and Bochkarev, A. (2002) *EMBO J.* **21,** 1855–1863
6. Binz, S. K., Sheehan, A. M., and Wold, M. S. (2004) *DNA Repair (Amst.)* **3,** 1015–1024
7. Kelman, Z., and O'Donnell, M. (1995) *Nucleic Acids Res.* **23,** 3613–3620
8. Wyman, C., and Botchan, M. (1995) *Curr. Biol.* **5,** 334–337
9. Fien, K., and Stillman, B. (1992) *Mol. Cell. Biol.* **12,** 155–163
10. Krishna, T. S., Kong, X. P., Gary, S., Burgers, P. M., and Kuriyan, J. (1994) *Cell* **79,** 1233–1243
11. Yuzhakov, A., Kelman, Z., Hurwitz, J., and O'Donnell, M. (1999) *EMBO J.* **18,** 6189–6199
12. Tsurimoto, T., and Stillman, B. (1991) *J. Biol. Chem.* **266,** 1961–1968
13. Maga, G., and Hubscher, U. (2003) *J. Cell Sci.* **116,** 3051–3060
14. Warbrick, E. (2000) *BioEssays* **22,** 997–1006
15. Zou, Y., Liu, Y., Wu, X., and Shell, S. M. (2006) *J. Cell. Physiol.* **208,** 267–273
16. Cullmann, G., Fien, K., Kobayashi, R., and Stillman, B. (1995) *Mol. Cell. Biol.* **15,** 4661–4671
17. Neuwald, A. F., Aravind, L., Spouge, J. L., and Koonin, E. V. (1999) *Genome Res.* **9,** 27–43
18. Kim, J., and MacNeill, S. A. (2003) *Curr. Biol.* **13,** R873–R875
19. Majka, J., and Burgers, P. M. (2004) *Prog. Nucleic Acids Res. Mol. Biol.* **78,** 227–260
20. Zernik-Kobak, M., Vasunia, K., Connelly, M., Anderson, C. W., and Dixon, K. (1997) *J. Biol. Chem.* **272,** 23896–23904
21. Wu, X., Shell, S. M., and Zou, Y. (2005) *Oncogene* **24,** 4728–4735
22. Hoege, C., Pfander, B., Moldovan, G. L., Pyrowolakis, G., and Jentsch, S. (2002) *Nature* **419,** 135–141
23. Stelter, P., and Ulrich, H. D. (2003) *Nature* **425,** 188–191
24. Kannouche, P. L., Wing, J., and Lehmann, A. R. (2004) *Mol. Cell* **14,** 491–500
25. Watanabe, K., Tateishi, S., Kawasuji, M., Tsurimoto, T., Inoue, H., and Yamaizumi, M. (2004) *EMBO J.* **23,** 3886–3896
26. Friedberg, E. C., Lehmann, A. R., and Fuchs, R. P. (2005) *Mol. Cell* **18,** 499–505
27. Bienko, M., Green, C. M., Crosetto, N., Rudolf, F., Zapart, G., Coull, B., Kannouche, P., Wider, G., Peter, M., Lehmann, A. R., Hofmann, K., and Dikic, I. (2005) *Science* **310,** 1821–1824
28. Shiomi, Y., Shinozaki, A., Nakada, D., Sugimoto, K., Usukura, J., Obuse, C., and Tsurimoto, T. (2002) *Genes Cells* **7,** 861–868
29. Fukuda, K., Morioka, H., Imajou, S., Ikeda, S., Ohtsuka, E., and Tsurimoto, T. (1995) *J. Biol. Chem.* **270,** 22527–22534
30. Masuda, Y., Suzuki, M., Piao, J., Gu, Y., Tsurimoto, T., and Kamiya, K. (2007) *Nucleic Acids Res.* **35,** 6904–6916
31. Henricksen, L. A., Umbricht, C. B., and Wold, M. S. (1994) *J. Biol. Chem.* **269,** 11121–11132
32. Honda, R., Tanaka, H., and Yasuda, H. (1997) *FEBS Lett.* **420,** 25–27
33. Imai, N., Kaneda, S., Nagai, Y., Seno, T., Ayusawa, D., Hanaoka, F., and Yamao, F. (1992) *Gene (Amst.)* **118,** 279–282
34. Harrison, S. D., Solomon, N., and Rubin, G. M. (1995) *Genetics* **139,** 1701–1709
35. Haas, A. L., and Bright, P. M. (1988) *J. Biol. Chem.* **263,** 13258–13267
36. Fiser, A., and Sali, A. (2003) *Methods Enzymol.* **374,** 461–491
37. Tomii, K., and Akiyama, Y. (2004) *Bioinformatics (Oxf.)* **20,** 594–595
38. Koradi, R., Billeter, M., and Wuthrich, K. (1996) *J. Mol. Graph.* **14,** 29–32
39. Bowman, G. D., Goedken, E. R., Kazmirski, S. L., O'Donnell, M., and Kuriyan, J. (2005) *FEBS Lett.* **579,** 863–867
40. Kim, H. S., and Brill, S. J. (2001) *Mol. Cell. Biol.* **21,** 3725–3737
41. Bowman, G. D., O'Donnell, M., and Kuriyan, J. (2004) *Nature* **429,** 724–730
42. Motegi, A., Sood, R., Moinova, H., Markowitz, S. D., Liu, P. P., and Myung, K. (2006) *J. Cell Biol.* **175,** 703–708
43. Unk, I., Hajdu, I., Fatyol, K., Szakal, B., Blastyak, A., Bermudez, V., Hurwitz, J., Prakash, L., Prakash, S., and Haracska, L. (2006) *Proc. Natl. Acad. Sci. U. S. A.* **103,** 18107–18112
44. Gomes, X. V., and Burgers, P. M. (2001) *J. Biol. Chem.* **276,** 34768–34775
45. Podust, V. N., Tiwari, N., Stephan, S., and Fanning, E. (1998) *J. Biol. Chem.* **273,** 31992–31999
46. Moldovan, G. L., Pfander, B., and Jentsch, S. (2007) *Cell* **129,** 665–679
47. Wyatt, M. D., and Pittman, D. L. (2006) *Chem. Res. Toxicol.* **19,** 1580–1594
48. Stojic, L., Brun, R., and Jiricny, J. (2004) *DNA Repair (Amst.)* **3,** 1091–1101
49. Trojan, J., Zeuzem, S., Randolph, A., Hemmerle, C., Brieger, A., Raedle, J., Plotz, G., Jiricny, J., and Marra, G. (2002) *Gastroenterology* **122,** 211–219
50. Hoeijmakers, J. H. (2001) *Nature* **411,** 366–374
51. Krokan, H. E., Nilsen, H., Skorpen, F., Otterlei, M., and Slupphaug, G. (2000) *FEBS Lett.* **476,** 73–77

16. ヒト REV1 による損傷乗り越え DNA 合成の生化学的解析

朴　金蓮・増田　雄司・神谷　研二

Ⅰ. 緒　　言

電離放射線は，DNA のさまざまな部位に作用し，酸化的 DNA 損傷を引き起こす。DNA 損傷の多くは，DNA 合成の際に正常な塩基対合を妨げることにより DNA 複製を強く阻害する。DNA 複製の阻害は細胞にとって致死的であるため，これを回避するための細胞応答機構が重要な役割をもつ。損傷乗り越え DNA 合成（translesion synthesis, TLS）機構は，損傷特異的な DNA ポリメラーゼが，損傷部位での DNA 合成反応を行い，DNA 複製を回復する機能を持つ。TLS は DNA 損傷に対する細胞応答の一つであり，DNA 修復機構とともに染色体の恒常性維持に必要不可欠な生物機能である。

酵母で同定された *REV* 遺伝子群は TLS に関与し，放射線による突然変異の誘発に重要な役割を担っている[1]。われわれはこれまでに，REV1 タンパク質は，*umuC/dinB/XPV* ファミリーの遺伝子がコードする Y ファミリー損傷乗り越え型 DNA ポリメラーゼに属し，酸化的 DNA 損傷の TLS を効率よく行うことを明らかにした[2)-5)]。

色素性乾皮症の原因遺伝子である *XPV* がコードする pol η は同じ Y ファミリーに属し，紫外線による DNA 損傷の一つであるチミンダイマーに対して正しく dAMP を取り込み，損傷部位を正しく乗り越える[6]。一方，REV1 には DNA ポリメラーゼ活性はなく，酸化的 DNA 損傷に対して唯一 dCMP を取り込む[1]。この活性は進化的にとてもよく保存されていることから，損傷部位に対する dCMP の取り込みが，生体防御において重要な活性であることが示唆されているが，その生物学的意義は今のところ不明である。

当研究室では，これまでに，ヒト REV1 タンパク質による損傷乗り越え DNA 合成の分子機構を明らかにするため，組み換え REV1 タンパク質を精製し，その生化学的解析を行ってきた。REV1 は鋳型 G に対して，dCMP，dGMP，dTMP を挿入し，dCMP を取り込む反応が最も効率高いことが明らかとなった。また，鋳型 A，T，C に対して dCMP を挿入し，電離放射線によって生じる DNA 損傷の一つ，脱塩基部位（AP site）に対して，dCMP を効率よく取り込むことが分かった。今回われわれは上述の鋳型以外に，酸化的 DNA 損傷により生ずる U（ウラシル），8-オキソグアニン（8-oxoguanine），またアルキル化剤により生じる O^6-メチルグアニン（O^6-methylguanine）など損傷部位を持つ鋳型を使って，REV1 の損傷乗り越え活性を調べた。その結果，REV1 はさまざまな，損傷部位に dCMP を効率的に取り込むことで，DNA 損傷乗り越え活性を持つことが分かった。

Ⅱ. 材料と方法

組み換え REV1 タンパク質は，ヒスタグ融合タンパク質として大腸菌で過剰生産させた後，ニッケル親和性クロマトグラフィー，ゲル濾過クロマトグラフィーにより精製した。精製したタンパク質の dNMP 転移活性は，プライマー伸長反応として検出した[2)-5)]。

Ⅲ. 結　　果

REV1 の損傷鋳型塩基に対する基質特異性を測定するために，図 1 に示した U（ウラシル），脱塩基部位（AP site），O^6-メチルグアニン（O^6-methylguanine），8-オキソグアニン（8-oxoguanine）など鋳型 DNA を用いて dGTP，dATP，dTTP，dCTP それぞれまたは，4 種類の dNTP の存在下でプライマー伸長反応を行った。その結果，REV1 の鋳型 G に対して dCMP を選択的に取り込むのに対して，U（ウラシル），AP（脱塩基部位），G-6me（O^6-メチルグアニン），G-8oxo（8-オキソグアニン）に対しても dCMP を選択的に取り込むことが分かった。また，G-8oxo（8-オキソグアニン）に対しては，dGMP，dTTP も

JinLian Piao, Yuji Masuda, Kenji Kamiya: Biochemical analysis of deoxytidyl transferase axtivity of human REV1. Department of Experimental Oncology, Research Institute for Radiation Biology and Medicine, Hiroshima University.
広島大学原爆放射線医科学研究所ゲノム障害制御研究部門分子発がん制御研究分野

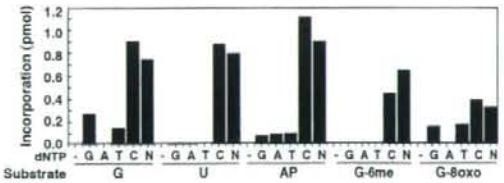

図 1　REV1 プライマー伸長反応産物の解析

図の横軸は，デオキシヌクレオチドと基質（substrate）を示している。5' 末端を ^{32}P で標識した 13-mer のプライマーと 30-mer の鋳型 DNA をアニーリングさせた。基質は G と損傷鋳型 DNA はそれぞれプライマー末端のすぐ下流の鋳型塩基 G，U（ウラシル），AP（脱塩基部位），G-6me（O^6-メチルグアニン），G-8oxo（8-オキソグアニン）に対するデオキシヌクレオチドの取り込みを測定することができる。上述の鋳型 DNA と REV1 を図に示した 4 種類の dNTP（G, A, T, C）のそれぞれ，またはそれらの混合物（N）の存在下でプライマー伸長反応を行い，反応産物を変性アクリルアミドゲル電気泳動し，オートラジオグラフィーにより解析した。(-) は dNTP なしのコントロール。図の縦軸は，デオキシヌクレオチドの取り込み効率を示している。

取り込むことが検出された。これらの結果から，ヒト REV1 は，損傷 DNA に対して dCMP を選択的に取り込むことで損傷を乗り越えることが実験的に証明された。

Ⅳ．考　　察

本研究でわれわれは，REV1 はさまざまな損傷部位に dCMP を効率的に取り込むことで，DNA 損傷を乗り越え活性を持つことが分かった。今後は，変異型 REV1 の損傷を乗り越え基質特異性の詳細な生化学解析を行い，dCMP transferase 活性の生物学的意義を明らかにしたいと考えている。

Ⅴ．結　　語

REV1 の損傷 DNA に対して dCMP を選択的に取り込むことで損傷を乗り越えることが実験的に証明された。

文　　献

1) Nelson JR, Lawrence CW, et al: Deoxycytidyl transferase activity of yeast REV1 protein, Nature: 382: 729–731, 1996.
Masutani C, Kusumoto, R et al: The XPV (xeroderma pigmentosum variat) gene encodes human DNA polymerase h, Nature: 399: 700–704, 1999.

2) Masuda Y, Takahashi M, et al: Deoxycytidyl transferase activity of the human REV1 protein is closely associated with the conserved polymerase domain, J Biol Chem: 276: 15051–15058, 2001.

3) Masuda Y, Takahashi M, et al: Mechanisms of dCMP Transferase Reaction Catalyzed by Mouse Rev1 protein, J Biol Chem: 277: 3040–3046, 2002.

4) Masuda Y, Kamiya K: Biochemical properties of the human REV1 protein, FEBS Letters 520: 88–92, 2002.

5) Masuda Y, Ohmae M, et al: Structure and enzymatic properties of a stable complex of the human REV1 and REV7 proteins, J Boil Chem 278: 12356–12360, 2003.

6) Masutani C, Kusumoto R, et al: The XPV (xeroderma pigmentosum variant) gene encodes human DNA polymerase η, Nature: 399: 700–704, 1999.

RADIATION RESEARCH 170, 216–223 (2008)
0033-7587/08 $15.00

Absence of *Ku70* Gene Obliterates X-Ray-Induced *lacZ* Mutagenesis of Small Deletions in Mouse Tissues

Yoshihiko Uehara,[a] Hironobu Ikehata,[a] Jun-ichro Komura,[a] Ari Ito,[a] Masaki Ogata,[a] Tsunetoshi Itoh,[a] Ryoichi Hirayama,[b] Yoshiya Furusawa,[b] Koichi Ando,[b] Tatjana Paunesku,[c] Gayle E. Woloschak,[c] Kenshi Komatsu,[d] Shinya Matsuura,[e] Tsuyoshi Ikura,[a] Kenji Kamiya[e] and Tetsuya Ono[a,1]

[a] *Department of Cell Biology, Graduate School of Medicine, Tohoku University, 2-1 Seiryo-machi, Aoba-ku, Sendai 980-8575, Japan;* [b] *Heavy-Ion Radiobiology Research Group, National Institute of Radiological Sciences, Anagawa 4-9-1, Inage-ku, Chiba 263-8555, Japan;* [c] *Department of Radiology, Feinberg School of Medicine, Northwestern University, Chicago, IL 60611;* [d] *Department of Genome Repair Dynamics, Radiation Biology Center, Kyoto University, Yoshida-konoe, Sakyo-ku, Kyoto 606-8501, Japan; and* [e] *Research Institute for Radiation Biology and Medicine, Hiroshima University, Kasumi-ku, Hiroshima 734-8553, Japan*

Uehara, Y., Ikehata, H., Komura, J-I., Ito, A., Ogata, M., Itoh, T., Hirayama, R., Furusawa, Y., Ando, K., Paunesku, T., Woloschak, G. E., Komatsu, K., Matsuura, S., Ikura, T., Kamiya, K. and Ono, T. Absence of *Ku70* Gene Obliterates X-Ray-Induced *lacZ* Mutagenesis of Small Deletions in Mouse Tissues. *Radiat. Res.* 170, 216–223 (2008).

With the goal of understanding the role of non-homologous end-joining repair in the maintenance of genetic information at the tissue level, we studied mutations induced by radiation and subsequent repair of DNA double-strand breaks in *Ku70* gene-deficient *lacZ* transgenic mice. The local mutation frequencies and types of mutations were analyzed on a *lacZ* gene that had been chromosomally integrated, which allowed us to monitor DNA sequence alterations within this 3.1-kbp region. The mutagenic process leading to the development of the most frequently observed small deletions in wild-type mice after exposure to 20 Gy of X rays was suppressed in *Ku70*$^{-/-}$ mice in the three tissues examined: spleen, liver and brain. Examination of DNA break rejoining and the phosphorylation of histone H2AX in *Ku70*-deficient and -proficient mice revealed that *Ku70* deficiency decreased the frequency of DNA rejoining, suggesting that DNA rejoining is one of the causes of radiation-induced deletion mutations. Limited but statistically significant DNA rejoining was found in the liver and brain of *Ku70*-deficient mice 3.5 days after irradiation, showing the presence of a DNA double-strand break repair system other than non-homologous end joining. These data indicate a predominant role of non-homologous end joining in the production of radiation-induced mutations *in vivo*. © 2008 by Radiation Research Society

INTRODUCTION

DNA double-strand breaks cause serious problems for cells because their presence leads to losses of small and large DNA fragments. Two kinds of DNA repair systems are known to work to rejoin these breaks: non-homologous end joining (NHEJ) and homologous recombination repair (HRR). In many higher organisms, NHEJ has been shown to play a major role in genome maintenance. NHEJ occurs through the collaboration of several proteins, including Ku70, Ku80, DNA-PKcs, ligase IV and Cernunnos-XLF (*1–6*). Inactivation of the NHEJ system by knocking out one of the key genes in this repair pathway results in severe health problems including immunodeficiency, developmental abnormalities, early cancer development, and premature aging. Among these, cancer and premature aging are assumed to be induced at least in part by genomic instability caused by the lack of repair of spontaneously occurring DNA double-strand breaks (*1–4, 7, 8*). However, this assumption is not clearly established. Genomic alterations induced by DNA double-strand breaks are grouped into two categories: (1) large-scale changes such as chromosomal fragmentation, rearrangement of large DNA fragments, and telomere defects; (2) alteration of DNA at the gene sequence level, resulting in gene mutations. Studies on chromosomal structures in untreated NHEJ-deficient cultured cells showed elevated levels of fragmented and translocated chromosomes (*9–11*). Untreated NHEJ-deficient mice with an inactivated *Ku80* gene, on the other hand, had a reduced level of spontaneous large-scale DNA rearrangements compared to wild-type mice as judged by a chromosomally integrated *lacZ* gene enclosed in plasmid DNA (*12*). The discrepancy could be explained by elimination of cells containing chromosomal rearrangements *in vivo* by apoptosis, although little evidence is available to support this. Irradiation of cultured cells induces chromosomal abnormalities, which become even more frequent in NHEJ-deficient cells (*13*). This finding was supported by biochemical analyses of DNA rejoining using pulsed-field gel electrophoresis combined with Southern blot analysis (*14*). NHEJ deficiency resulted in the suppression of rejoining of 50% of the

[1] Address for correspondence: Department of Cell Biology, Graduate School of Medicine, Tohoku University, 2-1 Seiryo-machi, Aoba-ku, Sendai 980-8575, Japan; e-mail: tono@mail.tains.tohoku.ac.jp.

radiation-induced DNA double-strand breaks—a finding that is in agreement with elevated chromosomal fragment formation in irradiated NHEJ-deficient cells (*13*). Interestingly, the remaining 50% of the breaks were rejoined correctly in both wild-type and NHEJ-deficient cells, indicating the presence of an error-free repair system working independently from NHEJ. The method, however, identifies DNA of Mbp sizes and does not detect DNA alterations of less than a few hundred kbp. Thus the correct rejoining in the context of these published studies does not reflect the degree of DNA sequence maintenance at the nucleotide level such as base substitutions and short-fragment DNA deletions and insertions. More detailed studies were done with mutation analysis. However, the mutation studies performed on the cultured cells for the effect of NHEJ deficiency were complicated. The spontaneous mutation levels of both the *TK* and *HPRT* genes were not affected by DNA-PKcs deficiency, and radiation-induced mutation was suppressed at the *TK* locus but not at the *HPRT* locus (*15*). Ku-deficient Chinese hamster cells were shown to be sensitive to mutation induction at the *HPRT* locus using bleomycin, a drug that induces DNA double-strand breaks (*16*). *In vivo* studies of the role of NHEJ for radiation-induced mutation of single genes have not been performed previously.

Previously, we studied the molecular nature of mutations induced by radiation in mouse tissues using a chromosomally integrated *lacZ* gene enclosed in lambda DNA as a marker, and we found that the predominant type of mutation was deletion of one to a few hundred base pairs (*17*). Similar results were observed subsequently in a gpt delta transgenic mouse (*18*). This type of mutation is shown to be produced through errors associated with NHEJ repair of DNA double-strand breaks that were created either in the process of DNA rearrangement of antigen-receptor genes (*19*) or by restriction enzyme-induced double-strand breaks (*20–22*). Therefore, we postulated that NHEJ could be responsible for the major type of mutation found in tissues as a consequence of radiation exposure. We analyzed mutant frequencies and the molecular nature of the mutants as well as rejoining of DNA breaks in *Ku70*-knockout *lacZ* transgenic mice. Since the genome maintenance system in each tissue is unique and DNA repair and the mutational burden vary among different tissues (*23–27*), we examined three tissues with different cell renewal properties: spleen, liver and brain.

MATERIALS AND METHODS

Mice

Muta™ mice, which harbor the *lacZ*-containing lambda phage genome as a transgene (*28*), were purchased from Covance Research Products, Denver, PA. The genetic background of the mice was a mixture of BALB/c and DBA/2 (*28*). The Muta™ mice were mated with $Ku70^{+/-}$ mice (*29*). F_1 mice of the $Ku70^{+/-}$, $lacZ^+$ genotype were selected and mated again to obtain $Ku70^{-/-}$, $lacZ^+$; $Ku70^{+/-}$, $lacZ^+$; and $Ku70^{+/+}$, $lacZ^+$ mice. The genotype of *Ku70* was determined by PCR as described previously (*29*). The PCR primers for *lacZ* were 5′-(-84)CACCCCAGGCTTTACACTTT (sense primer) and 5′-(2525)ATCAGCACCGCATCAGCAAG (antisense primer). The PCR conditions were 94°C for 4 min followed by 28 cycles of 94°C for 30 s, 55°C for 1 min and 72°C for 1 min and a final incubation at 72°C for 4 min (*30*).

Irradiation

Two-month-old mice were placed in a plastic box in which they could move freely and were irradiated with 20 or 50 Gy of X rays (200 kVp, 10 mA, filtered with 1 mm aluminum and 0.5 mm copper, 0.72 Gy/min, Shimadzu HF320, Kyoto, Japan). For the analysis of DNA fragmentation, mice were irradiated at a higher dose rate to minimize DNA rejoining during irradiation (220 kVp, 17 mA, filtered with 0.5 mm aluminum and 0.3 mm copper, 5.83 Gy/min). The tissues were harvested immediately (2 to 3 min), 1 h or 3.5 days after irradiation. The animal experiments were conducted according to the Guidelines for Animal Welfare and Experimentation at Tohoku University.

Mutation Assay

Mutant frequencies were determined at 3.5 days after irradiation. Genomic DNA was isolated from tissues by phenol extraction and mixed with lambda phage packaging extract (Transpack® Packaging Extract, Stratagene, La Jolla, CA). The number of phages retrieved containing the *lacZ* gene was estimated by the number of plaques that developed on *E. coli* strain C of galE⁻. The number of phages containing a mutated *lacZ* gene was counted as plaques observed in the presence of phenyl-β-D-galactose. Two or three $Ku70^{+/+}$ and $Ku70^{+/-}$ mice and three or four $Ku70^{-/-}$ mice were examined.

Sequencing of the mutant *lacZ* gene was done by a DNA sequencer (ABI PRISM™ 3100, Applied Biosystems, Foster City, CA), and the sequences obtained were compared to the nucleotide sequence of the wild-type *lacZ* gene. For the analysis of the mutation spectrum, two or more mutants showing identical characteristics to the other mutant found in the same DNA preparation were eliminated from counting to avoid a possible effect of replication of mutation. The details of this procedure were described previously (*24, 30*).

SFGE Analysis of DNA Breaks

To monitor DNA breaks and rejoining, static-field gel electrophoresis (SFGE) was used (*31*). A part of the spleen or liver or a longitudinal half of a brain was minced with a pair of scissors, dissolved in phosphate-buffered saline, pipetted about 10 times to disassociate cells, strained through a 40-μm mesh strainer (BD Falcon, Bedford, MA), and rinsed twice by centrifugation. The spleen cell density was adjusted to 2.5×10^7 cells/ml. The liver and brain cell suspensions were adjusted to $OD_{600} = 12$ using a spectrophotometer, because the cells were difficult to count. The cell suspension (15 μl) was embedded in 55 μl of 1.3% agarose and lysed with lysis buffer and proteinase K at 50°C, 24 h (CHEF Genomic DNA Plug Kits, Bio-Rad Laboratories, Hercules, CA). The DNA was electrophoresed for 36 h at 0.6 V/cm. The DNA remaining in the well and the DNA released into the gel were quantified after staining with ethidium bromide. The details of this procedure were described previously (*31*). The fraction of DNA released from the wells was used as a measure of DNA breaks.

Western Blot Analysis of γ-H2AX

Approximately 0.1 g of spleen or 0.3 g of liver was minced with a pair of scissors and homogenized in a glass homogenizer in lysis buffer containing 0.5% Triton X-100. For brain, a longitudinal half of a whole organ was used. The homogenized samples were centrifuged at 800*g* for 2 min, and the precipitated nuclei were rinsed again with lysis buffer. The nuclei were lysed with 1% of SDS, and the DNA was fragmented by sonication. After the insoluble material was pelleted, nuclear proteins were separated by 15% SDS-polyacrylamide gel electrophoresis, trans-